IOP Conf. Series: Journal of Physics: Conf. Series **940** (2018) 012018 doi:10.1088/1742-6596/940/1/012018

ν-driven winds from the remnant of binary neutron star mergers

A Perego

Institut für Kernphysik, Technische Universität Darmstadt, Schlossgartenstraße 2, D-64289 Darmstadt, Germany

E-mail: albino.perego@physik.tu-darmstadt.de

Abstract. We present a 3D hydrodynamic study of the neutrino-driven winds that emerge from the remnant of a neutron star merger, represented by a thick accretion disc orbiting around a massive neutron star. This strong baryonic wind is blown out by neutrino absorption on free baryons inside the disc. It expands within a few tens of ms along the original binary rotation axis. If the central object survives for at least 200ms, the mass ejected in the wind can reach 5% of the initial mass of the accretion disc. Due to the intense neutrino irradiation, matter ejected in the wind increases its electron fraction between 0.3 and 0.4, producing weak r-process nucleosynthesis yields. We predict a distinct UV/optical transient associated with the wind ejecta that peaks from a few hours to a few days after the merger.

1. Introduction

Binary compact objects coalesce due to the emission of gravitational waves (GWs), carrying away orbital angular momentum and energy [1]. In addition to be primary targets for terrestrial GW detectors, such as aLIGO and aVIRGO, compact binary mergers involving at least one neutron star (NS) are expected to copiously emit neutrinos of all flavours (ν's), with luminosities comparable to the ones of a core collapse supernova event [2]. After the discovery of the first double NS binary, its has been soon recognized that the decompression of cold NS matter in mergers can represent a favourable site for the production of the heaviest elements in the Universe, in particular of rapid neutron capture process (r-process) elements [3]. In these systems, the mutual tidal interaction and the actual collision between the compact objects expel a fraction of the original mass in a dense accretion disc around a black hole or a (possibly gravitational unstable) massive neutron star (MNS). A fraction of this matter can even become unbound within a few ms (*dynamic ejecta*). Interactions between ν's and matter in the remnant, as well as the secular evolution of the accretion disc, are also expected to unbind matter in the so-called *ν-driven wind* and in the *viscous ejecta*, respectively. The decay of radioactive elements in the different ejection channels can power electromagnetic (EM) transients [4], whose detection in association with GW signals can directly prove the link between compact binary merger and r-process nucleosynthesis. The possible detection of such an EM signal in the afterglow of two short gamma-ray-bursts has recently corroborated the idea that binary compact mergers are also the progenitors of these powerful burst [5, 6, 7].

In this proceeding, we explore the origin and the properties of the ν-driven wind that emerges from the remnant of a double binary neutron star merger [8].

2. Method

To study the aftermath of a binary neutron star merger and the development of a ν-driven wind, we set up a radiation-hydrodynamics (HD) simulation. We take our initial conditions from the final stages of an equal mass binary NS merger simulation. The coalescence has been studied using a smoothed-particle hydrodynamics (SPH) code [9], complemented by a multi-flavour neutrino leakage scheme. We map the SPH data 10 ms from the beginning of the merger into the equally-spaced Cartesian grid (resolution: 1 km) of our 3D Eulerian hydrodynamics code `FISH` [10]. Neutrino-matter interaction is implemented via a multi-energy, multi-flavor leakage scheme. It provides spectral neutrino cooling rates as smooth interpolations between diffusion and free-streaming emission rates. The obtained neutrino luminosities are used to compute neutrino particle densities in optically thin regions, via a ray-tracing algorithm. Neutrino absorption rates are finally computed as a product of the local neutrino absorptivity and particle density. We use the HS tabulated nuclear equation of state ([11]) with the TM1 parametrization. We place 10^5 tracer particles, i.e. passively advected Lagrangian particles, in the disc around the MNS to record the local properties of matter. After an initial relaxation phase of ~ 10 ms, when only neutrino cooling processes are considered, the system is evolved for ~ 200 ms under the influence of both neutrino cooling and heating. The adopted uniform grid ensures a high spatial resolution in the disc and in the dilute wind, but it is not enough for the dense MNS, characterized by large density gradients. Therefore, the innermost part of the MNS ($\rho > 10^{12}\,\mathrm{g\,cm^{-3}}$) is treated as a stationary, axisymmetric rotating object.

3. Results

3.1. Neutrino emission

Neutrinos diffusing from the MNS and from the innermost part of the disc power an intense neutrino luminosity. This luminosity is only slightly decreased during the first hundreds of ms, due to the large energy reservoir in the central compact object and to the intense accretion rate onto it ($\dot{M} \sim 0.5\,M_\odot\,\mathrm{s^{-1}}$). The high neutron richness of the disc favours positron capture and ν_e absorption on free neutrons. As a consequence, $\bar{\nu}_e$ luminosities and mean energies are larger than the ones for ν_e's ($E_{\nu_e} \approx 11\,\mathrm{MeV}$ and $E_{\bar{\nu}_e} \approx 15\,\mathrm{MeV}$, while $L_{\bar{\nu}_e} \approx 3 \times 10^{52}\,\mathrm{erg\,s^{-1}}$ and $L_{\nu_e} \approx 1.7 \times 10^{52}\,\mathrm{erg\,s^{-1}}$). $\nu_{\mu,\tau}$'s and $\bar{\nu}_{\mu,\tau}$'s, which decouple from matter at the edge of the MNS, i.e. much deeper than electron flavour neutrinos, have larger mean energies ($E_{\nu_{\mu,\tau}} \approx 18\,\mathrm{MeV}$) but lower luminosities ($L_{\nu_{\mu,\tau}} \approx 9 \times 10^{51}\,\mathrm{erg\,s^{-1}}$). Due to the larger opacity provided by the disc along the equatorial direction, the luminosity is highly anisotropic and the isotropised luminosities in the polar direction are up to 3 times larger than the ones in the equatorial plane.

3.2. Wind dynamics and properties

A few tens of milliseconds after the beginning of the simulations, a low density wind develops from the disc (figure 1, see also [12]). The energy and momentum deposition operated by ν_e's and $\bar{\nu}_e$'s in the low density part of the disc ($\rho \lesssim 10^{10}\,\mathrm{g\,cm^{-3}}$) expand the merger debris and drives matter orbiting around the MNS on wider trajectories on the time scale of a few orbital periods. The wind originates mainly from the region of the disc located 50-100 km from the MNS and expands far from it, initially parallel to the rotational axis. As the distance from the central compact object increases, the vertical motion turns into a radial expansion. The ν irradiation of the initially extreme neutron rich matter in the disc changes the electron fraction in the wind. In particular, the dominant ν_e absorption on free neutrons rises Y_e towards larger values, ($Y_e \approx 0.42$). The entropy in the wind is initially increased by the ν energy deposition, before the expansion proceeds almost adiabatically. The evolution of the density and Y_e inside the wind can be seen in figure 2. Around 100 ms after the beginning of the simulation, the disc and the wind have reached a quasi-stationary state. While matter in the wind expands and cools, the free protons form first α-particles and, later at NSE freeze-out, neutron-rich heavy

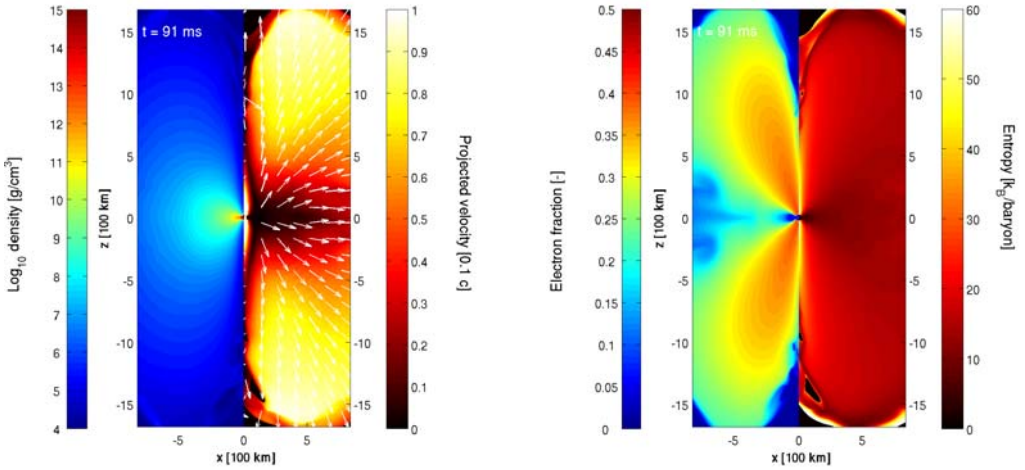

Figure 1. 2D slices ($y = 0$ plane) of the 3D simulation box of relevant quantities taken 90 ms after the beginning of our simulations. In the left figure, we represent the density (left) and the projected velocity (right). In the right figure, the electron fraction (left) and the entropy (right).

nuclei surrounded by free neutrons (with an initial density of $n_n \sim 10^{30}\,\mathrm{cm}^{-3}$). The associated release of nuclear binding energy is crucial to ultimately unbind matter in the wind.

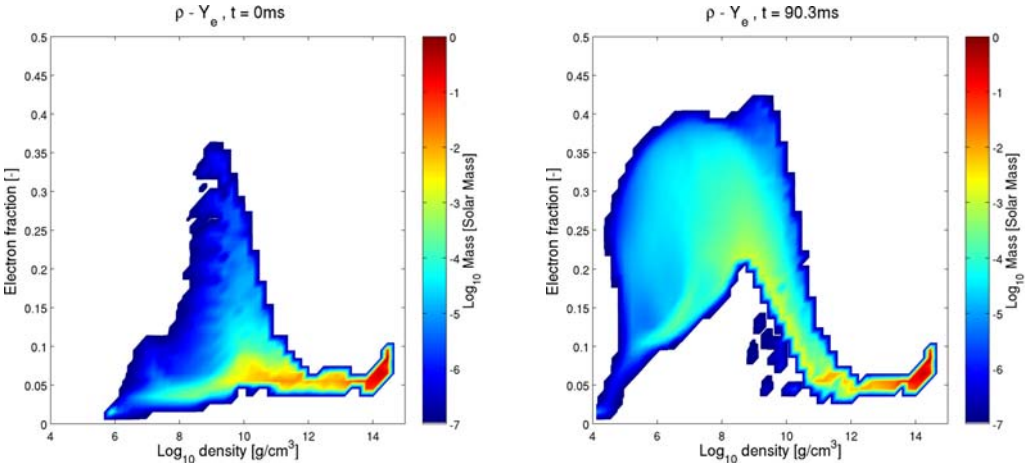

Figure 2. 2D histograms of density-Y_e conditions occurring inside our computational domain at $t = 0\,\mathrm{ms}$ (left) and at $t = 90\,\mathrm{ms}$ (right). Color coded is the amount of mass that experiences the thermodynamical conditions indicated by the location on the plane, at a given time. The development of the wind is visible in the right panel, where an increasing amount of matter is expanding at lower density ($\rho \lesssim 10^{10}\mathrm{g\,cm}^{-3}$) with higher Y_e, due to ν-matter interactions.

3.3. Wind ejecta, nucleosynthesis and EM signal

After 100 ms, $\sim 2 \times 10^{-3} M_\odot$ of matter in the wind has become unbound, while at 200 ms the mass of the ejecta has increased up to $\sim 9 \times 10^{-3} M_\odot$. This corresponds to 1% and 5% of the initial mass of the disc, respectively. Due to the stronger ν irradiation, matter expanding closer to the rotational axis has a larger electron fraction, closer to the equilibrium value. At early times ($t \lesssim 100\,\mathrm{ms}$), the competition between the expansion and the weak equilibrium time scales produces a wide spread of Y_e in the ejecta, ranging from 0.2 to 0.4. At later times, the prolonged

ν irradiation increases the electron fraction towards larger mean values ($Y_e \sim 0.33$) and reduces the relevant Y_e interval between 0.3 and 0.4. The velocities of the ejecta in the wind are non-relativistic and span a broad range between $0.06c$ and $0.1c$, while the entropy is usually between 15 and 20 $k_{\rm b}\,{\rm baryon}^{-1}$. The larger values for both the expansion velocity and the entropy are reached close to the rotational axis, where the neutrino influence is larger. We analyse the ejected tracer particles and we post-process them using a full nuclear reaction network. We obtain a weak r-process, characterized by the production of elements in the mass range $80 < {\rm A} < 130$, and a negligible fraction of lanthanides and actinides [13]. The combination of these ejecta with the yields expected from the dynamic ejecta [14, 15, 16, 19], and from the viscous evaporation of the disc [17, 18], indicates that neutron star mergers can be (one of) the astrophysical site(s) for the full r-process nucleosynthesis. We also calculate the EM signal expected from the wind ejecta [13]. We predict luminosity peaks in the range between 4 hours and 4 days after the merger, bluer than the IR peak expected from the dynamic ejecta around 10 days after the merger [20, 21].

4. Conclusions

We have shown that the ν's emitted from the remnant of a binary NS merger can trigger the formation of a baryonic wind within a few tens of ms after a binary NS merger. This wind has potentially relevant implications for the nucleosynthesis and for the EM transient expected from these compact binary mergers. Further investigations, including, for example, GR or more accurate neutrino treatments, are required to sharpen our understanding of this scenario.

Acknowledgments

AP gratefully acknowledges support by the Nuclear Astrophysics Virtual Institute to participate in Nuclear Physics in Astrophysics VII Conference, and the use of computational resources provided by the Swiss SuperComputing Center (CSCS), under the allocation grants s414. He also thanks D Martin and A Arcones for useful discussions.

References

[1] Peters P C 1964 *Phys. Rev.* **136** B1224
[2] Eichler D, Livio M, Piran T and Schramm D N 1978 *Nature* **340** 126
[3] Lattimer J M and Schramm D N 1974 *ApJ* **192** L145
[4] Li L and Paczyński B 1998 *ApJL* **507** L59
[5] Berger E, Fong W and Chornock R 2013 *ApJL* **774** L23
[6] Tanvir N R, Levan A J W, Fruchter A S, Hjorth J, Hounsell R A, Wiersema K and Tunnicliffe R L 2013 *Nature* **500** 547
[7] Yang B, Jin Z-P, Li X, Covino S, Zheng X-Z, Hotokezaka K, Fan Y-Z, Piran T and Wei D-M 2015 *Nature Communications* **6** 7323
[8] Perego A, Rosswog S, Cabezón R M, Korobkin O, Käppeli R, Arcones A and Liebendörfer M 2014 *MNRAS* **443** 3134
[9] Rosswog S and Price D 2007 *MNRAS* **379** 915
[10] Käppeli R, Whitehouse S, Scheidegger S, Pen U-L and Liebendörfer M 2011 *ApJS* **195** 20
[11] Hempel M and Schaffner-Bielich J 2011 *Nucl. Phys. A* **837** 210
[12] Dessart L, Ott C D, Burrows A, Rosswog S and Livne E 2009, *ApJ* **690** 1681
[13] Martin D, Perego A, Arcones A, Thielemann F-K, Korobkin O and Rosswog S 2015, accepted by *ApJ* (*Preprint* arXiv:1506.05048)
[14] Korobkin O, Rosswog S, Arcones A and Winteler C 2012, *MNRAS* **426** 1940
[15] Bauswein A, Goriely S and Janka H-T 2013, *ApJ* **773** 78
[16] Hotokezaka K, Kiuchi K, Kyutoku K, Muranuchi T, Sekiguchi Y, Shibata M, Taniguchi K 2013, *Phys. Rev. D* **88** 044026
[17] Fernández R and Metzger B 2013, *MNRAS* **435** 502
[18] Just O, Bauswein A, Pupillo R A, Goriely S and Janka H-T 2015, *MNRAS* **448** 541
[19] Wanajo S, Sekiguchi Y, Nishimura N, Kiuchi K, Kyutoku K, Shibata M 2014, *ApJL* **789** L39
[20] Metzger B and Fernández R 2014, *MNRAS* **441** 3444
[21] Grossman D, Korobkin O and Rosswog S 2014, *MNRAS* **439** 757